biomedicines

MDPI

Article

The Use of Machine Learning Algorithms and the Mass Spectrometry Lipidomic Profile of Serum for the Evaluation of Tacrolimus Exposure and Toxicity in Kidney Transplant Recipients

Dan Burghelea [1,2,†], Tudor Moisoiu [1,2,3,†], Cristina Ivan [4,†], Alina Elec [1], Adriana Munteanu [1], Ștefania D. Iancu [5], Anamaria Truta [6], Teodor Paul Kacso [7], Oana Antal [1,8], Carmen Socaciu [9], Florin Ioan Elec [1,2,*] and Ina Maria Kacso [7]

1 Clinical Institute of Urology and Renal Transplantation, 400006 Cluj-Napoca, Romania; dr.danburghelea@gmail.com (D.B.); tmoisoiu@gmail.com (T.M.); dralinaelec@gmail.com (A.E.); munteana2@yahoo.com (A.M.); antal.oanna@gmail.com (O.A.)
2 Department of Urology, "Iuliu Hatieganu" University of Medicine and Pharmacy Cluj-Napoca, 400012 Cluj-Napoca, Romania
3 Biomed Data Analytics SRL, 400696 Cluj-Napoca, Romania
4 "Regina Maria" Hospital, 400117 Cluj-Napoca, Romania; dr.ivancristina@gmail.com
5 Faculty of Physics, Babeș-Bolyai University, 400084 Cluj-Napoca, Romania; stefania.iancu22@yahoo.ro
6 Research Center for Functional Genomics, Biomedicine and Translational Medicine, "Iuliu Haţieganu" University of Medicine and Pharmacy Cluj-Napoca, 400337 Cluj-Napoca, Romania; dr.amma.truta@gmail.com
7 Department of Nephrology, "Iuliu Hatieganu" University of Medicine and Pharmacy Cluj-Napoca, 400012 Cluj-Napoca, Romania; teokacso@gmail.com (T.P.K.); inakacso@yahoo.com (I.M.K.)
8 Department of Anesthesiology, "Iuliu Hatieganu" University of Medicine and Pharmacy Cluj-Napoca, 400012 Cluj-Napoca, Romania
9 Faculty of Food Science and Technology, University of Agricultural Science and Veterinary Medicine Cluj-Napoca, Calea Mănăştur 3–5, 400372 Cluj-Napoca, Romania; csocaciudac@gmail.com
* Correspondence: ioan.elec@umfcluj.ro; Tel.: +40-756285972
† These authors contributed equally to this work.

check for updates

Citation: Burghelea, D.; Moisoiu, T.; Ivan, C.; Elec, A.; Munteanu, A.; Iancu, Ș.D.; Truta, A.; Kacso, T.P.; Antal, O.; Socaciu, C.; et al. The Use of Machine Learning Algorithms and the Mass Spectrometry Lipidomic Profile of Serum for the Evaluation of Tacrolimus Exposure and Toxicity in Kidney Transplant Recipients. *Biomedicines* **2022**, *10*, 1157. https://doi.org/10.3390/biomedicines10051157

Academic Editor: Gener Ismail

Received: 29 April 2022
Accepted: 14 May 2022
Published: 17 May 2022

Publisher's Note: MDPI stays neutral with regard to jurisdictional claims in published maps and institutional affiliations.

Abstract: Tacrolimus has a narrow therapeutic window; a whole-blood trough target concentration of between 5 and 8 ng/mL is considered a safe level for stable kidney transplant recipients. Tacrolimus serum levels must be closely monitored to obtain a balance between maximizing efficacy and minimizing dose-related toxic effects. Currently, there is no specific tacrolimus toxicity biomarker except a graft biopsy. Our study aimed to identify specific serum metabolites correlated with tacrolinemia levels using serum high-precision liquid chromatography–mass spectrometry and standard laboratory evaluation. Three machine learning algorithms were used (Naïve Bayes, logistic regression, and Random Forest) in 19 patients with high tacrolinemia (8 ng/mL) and 23 patients with low tacrolinemia (5 ng/mL). Using a selected panel of five lipid metabolites (phosphatidylserine, phosphatidylglycerol, phosphatidylethanolamine, arachidyl palmitoleate, and ceramide), Mg^{2+}, and uric acid, all three machine learning algorithms yielded excellent classification accuracies between the two groups. The highest classification accuracy was obtained by Naïve Bayes, with an area under the curve of 0.799 and a classification accuracy of 0.756. Our results show that using our identified five lipid metabolites combined with Mg^{2+} and uric acid serum levels may provide a novel tool for diagnosing tacrolimus toxicity in kidney transplant recipients. Further validation with targeted MS and biopsy-proven TAC toxicity is needed.

Keywords: tacrolimus; kidney transplant; metabolomic biomarkers; nephrotoxicity; machine learning; kidney graft function; liquid chromatography–mass spectrometry

1. Introduction

Kidney transplantation (KTx) is considered the gold-standard treatment for end-stage renal disease, providing a better quality of life and a higher survival rate than chronic dialysis [1,2].

The clinical management of patients who undergo renal transplants is challenging. Although surgical techniques have undergone significant advances in the past decade, the complexity of the immunological mechanisms involved, the poor quality of graft allocation strategies, and many knowledge gaps with respect to the personalization of immunosuppression therapies are responsible for significant differences in terms of graft survival [3,4]. To fill these gaps, tacrolimus (TAC), a calcineurin inhibitor (CNI), was introduced as a first-line chronic immunosuppression treatment alongside mycophenolate and steroid drugs. Even though TAC is 10–100 times more efficient than cyclosporine (a member of the CNI family) [5,6], the first two major clinical trials after the introduction of TAC in KTx show high rates of acute rejection (AR) in the first year after KTx (14–31%) [7,8], alongside a high percentage of toxicity events (39% nephrotoxicity, 6% neuropathy, 10% paresthesia, 13% diabetes mellitus, and 36% hyperglycemia) [7].

For each transplanted patient, it is well known that maintaining the perfect TAC blood concentration is a challenge due to pharmacodynamic and pharmacokinetic variations. Therefore, this translates into a narrow therapeutic window for TAC, which may put patients at risk for toxicity or graft rejection [9].

The current strategy for differentiating TAC nephrotoxicity and AR is based on TAC levels and serum creatinine evaluation. Unfortunately, these two parameters are suboptimal since patients with normal TAC levels may face increased creatine levels because of nephrotoxicity or AR. In this case, the current protocols call for the use of a graft biopsy, an invasive procedure, with TAC nephrotoxicity being an exclusion diagnostic [10]. For this reason, the search for novel biomarkers associated with TAC nephrotoxicity is intense, with most studies focusing on the identification of protein biomarkers in urine and serum, such as urinary NGAL, cystatin C, glutathione transferase, serum β-2 microglobulin, and α-1 microglobulin [11]. Unfortunately, none of them have managed to translate into practice [10].

Metabolomics, via high-performance liquid chromatography coupled with mass spectrometry (UHPLC–MS), offers new opportunities for the high-throughput measurement of large numbers of small molecules (<1500 Da), profiling the metabolites and identifying the most relevant ones by multivariate statistics, with possible clinical relevance.

Aside from the polar metabolites mentioned above, increasing consideration has recently been paid to the impact of tacrolimus on the lipid metabolism. For these reasons, in this study, we aimed to evaluate serum metabolomic and biochemical profiles of kidney graft recipients with outranged TAC levels (<5 ng/mL vs. >8 ng/mL), using untargeted lipidomic investigation by UHPLC–MS and machine learning algorithms; this strategy could be used for differential diagnostics of TAC toxicity (due to high TAC levels) and AR (due to insufficient TAC levels).

2. Materials and Methods

For this prospective transversal study, we enrolled 135 stable (defined as a creatinine level variation below 25% of the mean creatinine value), consecutive outpatients who underwent a KTx in our institution and for whom we performed standard follow-up between May 2020 and July 2020 at the Clinical Institute of Urology and Renal Transplantation Cluj-Napoca. The inclusion criteria were patients diagnosed with end-stage renal disease who underwent kidney transplantation with a TAC-based immunosuppressive therapy protocol (Advagraf 0.075–0.3 mg/kg/day), at least six months after the surgery. Patients with autoimmune diseases and those who developed lymphoproliferative disorders after kidney transplantation were excluded.

Clinical examinations, standard hematology, biochemistry panels, and tacrolinemia analyses were performed on all patients. Patients with outranged tacrolinemia (<5 or >8 ng/mL) were selected for metabolic profiling, as depicted in the workflow (Figure 1).

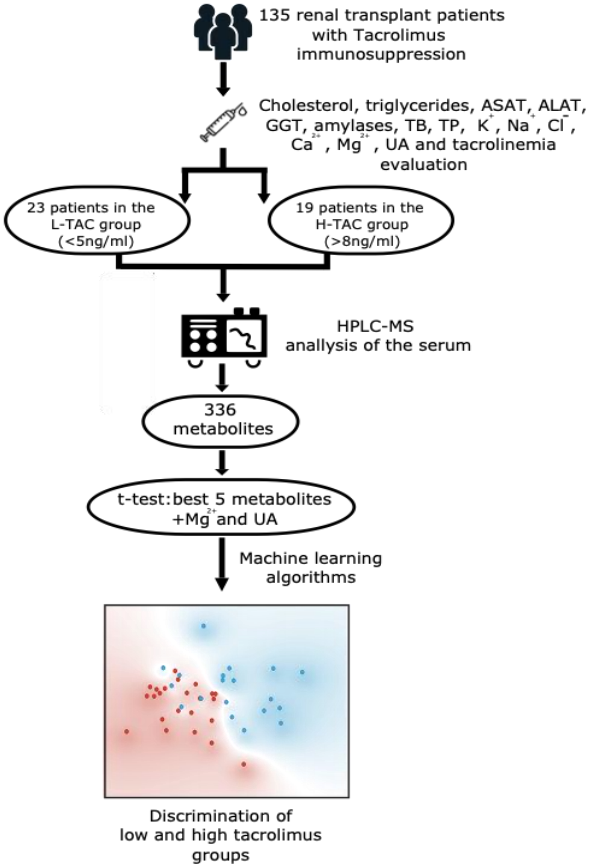

Figure 1. Workflow of the study. Abbreviations: ASAT—aspartate aminotransferase; ALAT—alanine aminotransferase; GGT—gamma-glutamyl transferase; TB—total bilirubin; TP—total proteins; K^+—potassium; Na^+—sodium; Cl^-—chloride; Ca^{2+}—ionized calcium; Mg^{2+}—magnesium; UA—uric acid; L-TAC—low tacrolinemia group; H-TAC—high tacrolinemia group; UHPLC–MS—high-precision liquid chromatography–mass spectrometry analysis.

We defined the patients with outranged TAC levels over 8 ng/mL as the TAC high-level group (H-TAC) and the patients who had low-level TAC under 5 ng/mL as the TAC low-level group (L-TAC).

2.1. Sample Processing

Blood samples were collected from patients at 24 h post-dosing of Advagraf, just prior to the next dose. Patients had fasted for a minimum of 8 h.

The serum samples were collected by vein puncture into vacutainer tubes without anticoagulants. The blood serum was separated by centrifugation at 2000× *g* for 10 min, and aliquots of 1 mL were stored at −80 °C until analysis was performed. An 0.8 mL mixture of methanol and acetonitrile (1:1) was added to 0.2 mL of serum to precipitate the protein content; the mixture was then vortexed for 1 min, maintained at 4 °C for 6 h, and then vortexed again for 1 min. After mixing, the vials were centrifuged at 12,500× *g* for 5 min, and the supernatant was collected and filtered through 0.2 µm nylon filters.

2.2. Laboratory Tests

Tacrolinemia was measured using semi-automated electrochemiluminescence immunoassays using the ArchitectPlus CI4100 automatic analyzer. Prior to the initiation of

the automated Architect sequence, a manual pretreatment step was performed in which the whole blood sample was extracted with a precipitation reagent and centrifuged. The supernatant was decanted into a Transplant Pretreatment Tube, which was placed onto the Architect iSystem [12,13].

The standard laboratory evaluation using the ArchitectPlus CI4100 automatic analyzer included serum cholesterol, triglycerides, glycemia, aspartate aminotransferase (ASAT), alanine aminotransferase (ALAT), gamma-glutamyl transferase (GGT), amylases, total proteins (TP), potassium (K^+), sodium (Na^{2+}), chloride (Cl^-), ionized calcium (Ca^{2+}), magnesium (Mg^{2+}), and uric acid (UA). Renal function was determined via the estimated glomerular filtration rate (eGFR), using the creatinine-based CKD-EPI equation [14,15].

The metabolomic serum profile was analyzed using high-precision liquid chromatography (UHPLC)–mass spectrometry (MS) analysis.

The UHPLC–MS analysis was performed on a Bruker Daltonics MaXis Impact (Bruker GmbH, Bremen, Germany) device that comprised a Thermo Scientific UHPLC UltiMate 3000 system with a Dionex Ultimate quaternary pump delivery and ESI+-QTOF-MS detection device on a C18 reverse-phase column (Acuity, UPLC C18 BEH, Dionex) (5 µm, 2.1 × 75 mm) at 25 °C and with a flow rate of 0.3 mL/min. The injection volume was 5.0 µL. The mobile phase was represented by a gradient of eluent A (water containing 0.1% formic acid) and eluent B (methanol: acetonitrile 1:1, containing 0.1% formic acid). The gradient system consisted of 99% A (min 0), 70% A (min 1), 40% A (min 2), 20% A (min 6), and 100%B (min 9–10), followed by 5 min with 99% A. The total running time was 15 min. The MS parameters were set for a mass range between 50 and 1000 Da. The nebulizing gas pressure was set at 2.8 bar, the drying gas flow at 12 L/min, and the drying gas temperature at 300 °C. Before each chromatographic run, a calibration with sodium formate was performed. Instrument control and data processing were performed using the TofControl 3.2, Hystar 3.2, and Data Analysis 4.2 software packages provided by Bruker Daltonics.

2.3. Statistical Methods

The metabolites identified by UHPLC–MS and from blood tests were ranked based on their ability to discriminate between the high- and low-tacrolinemia groups using the *t*-test feature selection method. The Student's *t*-test was applied for each metabolite, and the significance level was set to 0.05. The 5 statistically significant metabolites, along with the statistically significant blood parameters, were selected for further analysis. The classification accuracy for high and low tacrolinemia based on each significant metabolite was evaluated using a receiver operating characteristic curve for which the area under the curve (AUC) was calculated.

To quantitatively evaluate the multivariate classification power yielded by the biochemical blood parameters and the 5 significant metabolites, 3 independent machine learning algorithms (naive Bayes, logistic regression, and Random Forest) were trained to discriminate between the H-TAC and L-TAC groups. For logistic regression, the regularization type was set to Lasso and the C parameter to 140. For the Random Forest analysis, 10 trees were implemented. All the models were cross-validated using the leave-one-out method.

The inputs for the machine learning algorithms were either the biochemical blood parameters alone, the selected five metabolites alone, or all combined. For the classification based on the combined biochemical blood parameters and the five metabolites, data were normalized to unity prior to classification. The performance of the classification was assessed in terms of the AUC derived using receiver operating characteristic (ROC) analysis, classification accuracy, F1 score, precision, and recall. The quality performance metrics were represented as the average of the values from each repetition of the cross-validation.

Next, a principal component analysis (PCA) was performed to explore the dataset; the 5 metabolites along with the biochemical blood levels were used as inputs. For a better representation of the capacity to differentiate the TAC level of the experimental model, PCA was used to reduce the data dimensionality. The relationship between the number of

PCs and the explained variability in the original dataset is presented in Supplementary Figure S1.

For the correlation analysis, we used the Pearson correlation coefficient.

All statistical analyses were performed using the Quasar-Orange software (Bioinformatics Laboratory of the University of Ljubljana) [16,17].

The study was approved by the Ethics Committee of the Clinical Institute of Urology and Kidney Transplantation, Cluj-Napoca, No. 2/2020, and by the Ethics Committee of the Iuliu Hatieganu University of Medicine and Pharmacy in Cluj-Napoca, No. 285/2020. Written informed consent was obtained from all patients following the rules and principles of the Helsinki Declaration.

3. Results

Our dataset comprised 42 patients with outranged tacrolinemia levels; 19 and 23 patients had high (over 8 ng/mL) and low (under 5 ng/mL) levels of tacrolinemia, respectively, after KTx. The demographic data of the two groups are presented in Supplementary Table S1.

From the biochemistry panel, only Mg^{2+} and UA levels were changed to a statistically significant extent between the H-TAC and L-TAC groups, as depicted in Table 1.

Table 1. Student's *t*-test and area under the curve for standard follow-up biochemical blood tests were used to discriminate between patients with low and high tacrolinemia.

Blood Tests	H-TAC Mean ± SD	L-TAC Mean ± SD	*t*-Test (p)	AUC
Cholesterol (mg/dL)	228 ± 82	208 ± 39	0.237	0.56
Triglycerides (mg/dL)	172 ± 97	147 ± 70	0.349	0.56
Potassium (mmol/L)	4.4 ± 0.4	4.4 ± 0.6	0.725	0.51
Amylases (U/L)	93 ± 24	85 ± 30	0.312	0.58
Creatinine (mg/dL)	1.6 ± 0.5	1.6 ± 0.9	0.318	0.59
ASAT (U/L)	20 ± 7.2	19 ± 8.2	0.470	0.56
ALAT (U/L)	27 ± 15	20 ± 15	0.051	0.67
GGT (U/L)	34 ± 22	30 ± 20	0.294	0.59
TB (mg/dL)	0.72 ± 0.37	0.73 ± 0.29	0.740	0.53
Glycemia (mg/dL)	101 ± 16	117 ± 73	0.638	0.54
Total proteins (mg/dL)	7 ± 0.4	6.8 ± 0.4	0.341	0.58
Ca^{2+} (mmol/L)	4.6 ± 0.52	4.4 ± 0.4	0.116	0.64
Cl^{-} (mmol/L)	107 ± 2.7	106 ± 3.9	0.814	0.52
Na^{+} (mmol/L)	142 ± 2.5	141 ± 1.9	0.111	0.66
Mg^{2+} (mmol/L)	158 ± 15.52	178.4 ± 23.65	0.001	0.7243
UA (mg/dL)	72.42 ± 14.95	63.09 ± 10.57	0.025	0.6636

Using UHPLC–MS, 336 metabolites were identified (Supplementary Table S3 (Excel File S1) and Supplementary Table S2), from which only five were significantly related to over-ranged blood tacrolimus levels: phosphatidylserine 44:8 (PS), phosphatidylglycerol 36:6 (PG), phosphatidylethanolamine 36:4 (PE), arachidyl palmitoleate C36:1 (AP), and ceramide t18:0/22:0(2OH) (CER).

The Student's *t*-test and ROC analysis were used for the selection of the five statistically relevant metabolites (Table 2).

Table 2. Student's *t*-test and area under the curve for the significantly different metabolites used to discriminate between patients with low and high tacrolinemia. The mean levels of the metabolites represent peak UHPLC–MS intensities.

Metabolite	High Group Mean ± SD	Low Group Mean ± SD	*p*-Value	AUC
PS (counts)	245,714 ± 145,458	111,783 ± 52,986	0.01	0.818
AP (counts)	32,839 ± 11,132	42,818 ± 10,796	0.01	0.730
PG (counts)	273,380 ± 165,513	162,278 ± 115,156	0.02	0.724
PE (counts)	445,195 ± 419,624	197,051 ± 268,564	0.03	0.711
CER (counts)	464,002 ± 395,761	233,792 ± 263,222	0.03	0.807

Abbreviations: phosphatidylserine 44:8 (PS), phosphatidylglycerol 36:6 (PG), phosphatidylethanolamine 36:4 (PE), arachidyl palmitoleate C36:1 (AP), and ceramide t18:0/22:0(2OH) (CER).

The violin plots of the UHPLC–MS counts for the five selected metabolites and the serum concentrations of Mg^{2+} and UA are presented in Figure 2.

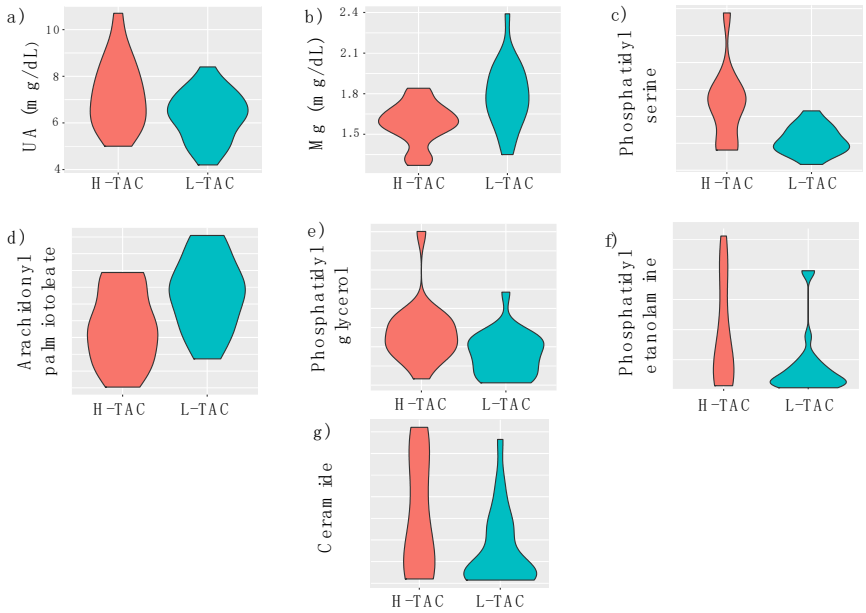

Figure 2. Violin plots of UA-uric acid (**a**), Mg^{2+}-magnesium (**b**), phosphatidyl serine (44:8) (**c**), arachidyl palmitoleate (C36:1) (**d**), phosphatidyl glycerol (36:6) (**e**), phosphatidyl ethanolamine (36:4) (**f**), and ceramide (t18:0/22:0(2OH)) (**g**), for the high-tacrolinemia (H-TAC) and low-tacrolinemia (L-TAC) groups.

Next, three machine learning algorithms (naïve Bayes, logistic regression, and Random Forest) were applied to evaluate the discrimination of the H-TAC and L-TAC groups using Mg^{2+}, UA, and the five metabolites. (Tables 3–5, Figure 3c).

Table 3. Head-to-head comparison of the area under the curve results for the classification accuracy yielded by magnesium and uric acid using three supervised classification algorithms.

Statistic Model	AUC	CA	F1	Precision	Recall
Naïve Bayes	0.621	0.578	0.579	0.585	0.577
Logistic regression	0.752	0.711	0.712	0.713	0.711
Random Forest	0.620	0.644	0.644	0.644	0.644

Abbreviations: AUC—area under the curve; CA—classification accuracy; F1 score; Precision-positive predictive value; Recall-sensitivity.

Table 4. Head-to-head comparison of the area under the curve results for the classification accuracy yielded by the five metabolites using three supervised classification algorithms.

Statistic Model	AUC	CA	F1	Precision	Recall
Naïve Bayes	0.750	0.667	0.667	0.683	0.667
Logistic regression	0.744	0.756	0.755	0.755	0.756
Random Forest	0.636	0.556	0.552	0.551	0.551

The five metabolites are phosphatidylserine 44:8, phosphatidylglycerol 36:6, phosphatidylethanolamine 36:4, arachidyl palmitoleate C36:1, and ceramide t18:0/22:0(2OH). Abbreviations: AUC—area under the curve; CA—classification accuracy; F1 score; Precision-positive predictive value; Recall-sensitivity.

Table 5. Head-to-head comparison of the area under the curve results for the classification accuracy yielded by magnesium, uric acid, and the five metabolites using three supervised classification algorithms.

Statistic Model	AUC	CA	F1	Precision	Recall
Naïve Bayes	0.799	0.756	0.756	0.764	0.756
Logistic regression	0.788	0.733	0.734	0.738	0.733
Random Forest	0.683	0.600	0.597	0.597	0.600

The five metabolites are phosphatidylserine 44:8, phosphatidylglycerol 36:6, phosphatidylethanolamine 36:4, arachidyl palmitoleate C36:1, and ceramide t18:0/22:0(2OH). Abbreviations: AUC—area under the curve; CA—classification accuracy; F1 score; Precision-positive predictive value; Recall-sensitivity.

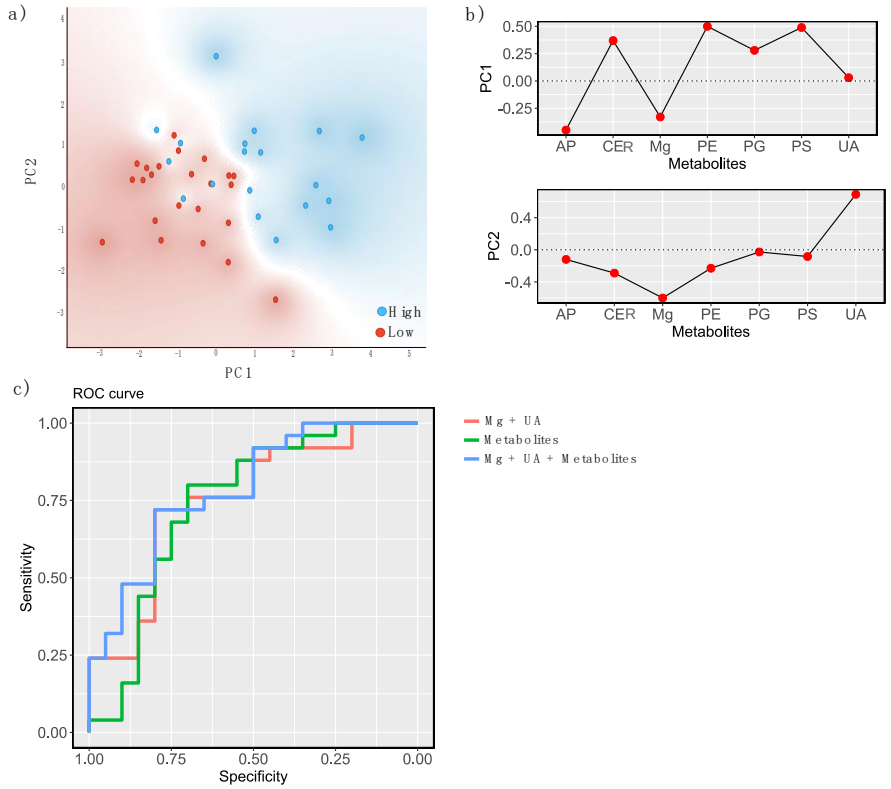

Figure 3. (**a**) The distribution of principal component (PC) score values (PC1 and PC2) of patients with metabolic profiles associated with low and high tacrolinemia. (**b**) Loading plots of the first two PCs yielded by PC analysis. (**c**) Head-to-head comparison of the receiver operating characteristic curves (ROC) for the classification accuracy yielded by magnesium, uric acid, the five metabolites (phosphatidylserine 44:8, phosphatidylglycerol 36:6, phosphatidylethanolamine 36:4, arachidyl palmitoleate C36:1, and ceramide t18:0/22:0(2OH)), and their combination using naïve Bayes analysis for supervised classification.

The distribution of score values following PCA of the H-TAC and L-TAC groups' metabolic profiles (PC1 and PC2) are represented in Figure 3a and show the clustering tendency of the H-TAC and L-TAC groups. Figure 3b presents the loading plot for PC1 and PC2, showing that CER, PE, PG, and PS are the variables that contribute the most to PC1, and UA and Mg^{2+} to PC2. Moreover, a negative correlation between Mg^{2+} and AP on the one hand and CER, PE, PG, and PS on the other hand is determined by the loading plot of PC1. By examining the score plot and loading plots pf PC1 and PC2, it is observed that the H-TAC group with positive values for PC1 has high values of CER, PE, PG, and PS, while the L-TAC group shows high values for Mg^{2+}, and AP.

Next, to evaluate the relation between the selected metabolites, we performed a correlation analysis between each metabolite, Mg^{2+}, and UA, using the Pearson correlation coefficient (Figure 4). We identified a statistically significant ($p < 0.05$) positive and moderate correlation between AP and Mg^{2+} and between CER and PE, and a high correlation between PE and PS. Between AP and PS, PE, and AP, we found statistically significant, moderate, and negative correlations, respectively.

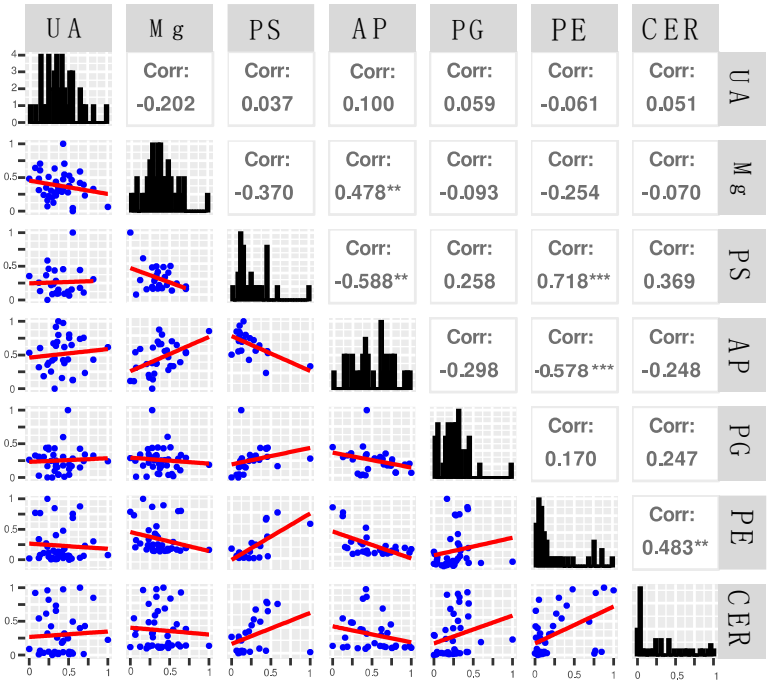

Figure 4. Correlation matrix and histogram between the metabolites, UA, and Mg^{2+}. Abbreviations and legend: UA–uric acid; Mg^{2+}–magnesium; phosphatidylserine 44:8 (PS), phosphatidylglycerol 36:6 (PG), phosphatidylethanolamine 36:4 (PE), arachidyl palmitoleate C36:1 (AP), and ceramide t18:0/22:0(2OH) (CER); Corr–Pearson correlation coefficient; ** $p < 0.01$; *** $p < 0.001$.

4. Discussion

In this current study, we use untargeted UHPLC–MS serum profiling and routine biological evaluation of the serum for the diagnosis of TAC toxicity. From 135 stable consecutive KTx recipient patients for whom TAC serum level was evaluated, we selected 19 patients with low tacrolinemia (<5 ng/mL) (L-TAC) and 23 patients with high tacrolinemia (>8 ng/mL) (H-TAC) (Figure 1).

The currently recommended standard immunosuppression therapy for patients undergoing KTx comprises CNI (preferably TAC because of its higher efficacy) combined with mycophenolate and steroids [6,18]. Because of the narrow therapeutic window of TAC therapeutic protocols, the transplanted patients are potentially at risk of underexposure and allograft rejection, or on the contrary, overexposure, and toxicity [19]. Consequently, the determination of serum TAC and creatinine is insufficient to assess the optimal systemic exposure.

From a pharmacokinetic point of view, tacrolimus is metabolized in the liver but also in the gut and kidney; this process is mediated by the phase I oxidase system via CYP3A4/5 [20,21] and the phase II metabolism by demethylation, glucuronidation, sulfation, acetylation, and conjugation. The metabolites are present in low concentrations in the blood and have minor pharmacological activity when compared to tacrolimus itself and are of minor clinical relevance [22].

Regarding the liver metabolization of TAC, its active metabolite, 6-mercaptopurine (6-MP), is metabolized via three different metabolic pathways. It can be inactivated by thiopurine methyltransferase to 6-metylmercaptopurine or by xanthine oxidase to 6-thiouric, or

it can be activated to 6-thioguanine nucleotide, which explains its therapeutic availability. TAC is primarily metabolized by the CYP3A enzyme system, which includes CYP3A5, CYP3A4, CYP3A7, and CYP3A43, and it is expressed in the small intestine, liver, and kidney [9,23,24].

In order to optimize the TAC therapeutic response, i.e., to minimize subtherapeutic and supratherapeutic TAC exposure in the immediate post-transplant phase, recent research studies aim to identify novel biomarkers correlated with TAC exposure; such biomarkers might provide an accurate algorithm to predict an individual's TAC starting dose and the therapeutic dosage required to improve clinical outcome in kidney transplant patients [25–27].

Experimental animal models show that there is a change in the metabolomic profile of urine after the administration of cyclosporine (decreased levels of succinate, citrate, and alpha-ketoglutarate, and increased levels of taurine) [28]. In contrast, time-related studies showed that, at 28 days after the administration of cyclosporine, there is a reduction in Krebs cycle intermediates and trimethylamine-N-oxide concentrations, whereas acetate, lactate, trimethylamine, and glucose concentrations increase [29]. These results were recently validated in humans [30]. Regarding TAC, to our knowledge, there is only one published study by Klepacki et al., who validated a panel of ten urine metabolites used in cyclosporine studies (glucose, hippurate, lactate, oxoglutarate, sorbitol, succinate, TMAO, UA, citrate, and creatinine) using targeted MS [31]. Interestingly, the result showed that, after three months, the level of the selected metabolites returned to normal, except for oxoglutarate, lactate, and uric acid [31]. It is unknown whether the level of the selected metabolite would change in case of TAC toxicity.

In our study, all the metabolites that differed between the H-TAC and L-TAC groups were components of the lipid metabolism. Kim et al. showed that the level of lipids increases after transplantation, especially in patients treated with cyclosporine A. Using proton nuclear magnetic resonance, they identified LDL, VLDL CH3, lipid CH2CH2CO, lipid CH2C=C, lipid CH2CO, and lipid CH as being upregulated [32]. Immunosuppressive therapy in KTx patients leads to the accumulation of triglyceride-enriched VLDL and LDL, increasing the atherosclerotic and cardiovascular risk for these patients [33–35].

Mechanisms of hyperlipidemia associated with CNI were more extensively studied with cyclosporine, which interferes with the binding of LDL cholesterol to the LDL receptor, bile acid synthesis, and 26 hydroxylase enzymes. In addition, cyclosporine is highly lipophilic and transported within the core of LDL cholesterol particles. In the process, it may change the molecular configuration of LDL. TAC generally provides a safer lipidic profile than cyclosporin, as cyclosporin new-onset hyperlipidemia remissions were reported after switching to TAC-based immunosuppression. However, the in-depth interactions of TAC with the lipid metabolome have not been extensively studied or applied in clinical practice [34,36,37].

Phosphatidyl glycerol, phosphatidylserine, phosphatidylethanolamine, and phosphatidylinositol (PI)-precursor of phosphatidylinositol 3-phosphate (PI3P) are cell membrane glycerophospholipids derived from the same glycerol backbone, namely diacylglycerol (DAG), as presented in Figure 5, and have different roles in biological membranes [38,39]. The pathway between CNI and induced changes in glycerophospholipid synthesis is still being studied, but CNI seems to inhibit the expression of phosphoinositide-3-kinase (PI3K) and other protein kinases as a mechanism of inducing nephrotoxicity [40]. In a recently published article, Karolin et al. showed that the CNI-induced nephrotoxic effect is obtained by an independent pathway from the known nuclear-activated T-cell (N-FAT) mechanism [40]. Thus, CNI seems to inhibit the expression of many protein kinases, including PI3K. The authors showed that blocking protein kinases in the tubular epithelial cells of the nephron leads to the increased expression of fibroblast growth factor–inducible 14 (Fn14), the receptor of TWEAK (TNF-related weak inducer of apoptosis), a key molecule involved in fibrosis and apoptosis in the kidney and renal graft [41]. Because CNI inhibits PI3K expression, there seems to be an accumulation of its substrate, PI3P and DAG, which are, in turn, metabolized in Phosphatidyl glycerol, phosphatidylserine, and

phosphatidylethanolamine (Figure 5), in line with our result that shows increased levels of PG, PS, and PE in the H-TAC group compared to the L-TAC group (Table 2). Further investigation of these hypotheses is needed.

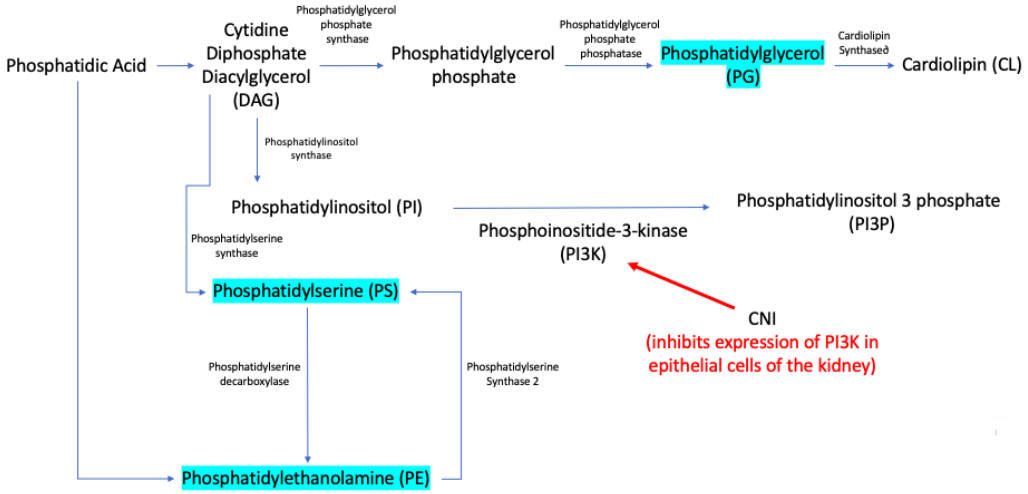

Figure 5. Lipid metabolic map.

Palmitic acid derivates were identified by our study as occurring in lower amounts in the H-TAC group, consistent with upregulation of the glycerophospholipid pathway to the detriment of the fatty acid/triglyceride pathway [42].

Ceramides are central molecules of the sphingolipid metabolism, with essential bioactive implications in cell processes such as apoptosis, necrosis, and autophagy-dependent cell death [43]. Increased levels of ceramides are strongly connected with the deterioration of pancreatic beta-cell function, insulin sensitivity, vascular reactivity, and mitochondrial metabolism; therefore, there are studies showing their presence in heart disease, atherosclerosis, hepatic disease, insulin resistance, and diabetes [44]. Concerning renal disease, ceramides and their metabolites are recognized as being part of the pathological mechanism in acute kidney injury, kidney cancer, polycystic kidney disease, and diabetic nephropathy [45]. In a recent study conducted on 760 patients, it was shown that increased levels of ceramides were on the direct axis of focal segmentary glomerulosclerosis [46]. These findings are in line with our results describing higher levels of ceramide t18:0/22:0(2OH) in the H-TAC group compared to the L-TAC group and also support a possible pathway for drug-induced nephrotoxicity.

After transplantation, Mg^{2+} serum levels decrease in part because the immunosuppressive therapy, especially CNI, increases Mg^{2+} urinary excretion. One study found that hypomagnesemia was observed in 6.6% of patients undergoing TAC therapy. On the other hand, hyperuricemia is a common complication in organ transplant recipients and is frequently associated with chronic immunosuppressive therapy (including TAC treatment), even though the role of UA levels in the survival of kidney grafts remains controversial [47–51].

There are few studies exploring metabolomics in kidney transplant patients. Previous studies that investigated allograft rejection and CNI-related side effects found that the metabolites were mainly represented by sugars, inositol, and hippuric acid [52]. These studies differed from ours in terms of the design and treatment explored (TAC).

Furthermore, metabolites such as tryptophan and arginine were previously identified as potential biomarkers for acute kidney injury with a high AUC when compared to creatinine; however, that study failed to associate direct toxicity with TAC [53].

There are several limitations to our study. The most important is the use of only untargeted MS because, for the mass implementation of the panel, cut-off values are mandatory. Additionally, there is no validation group with graft-biopsy-proven TAC toxicity. Another

limitation is the lack of analysis regarding the time from transplantation since previously published studies have shown that concentration changes in the metabolites related to oxidative stress are time-related [31].

For future research, we will use targeted MS to help establish a cut-off value for these metabolites, followed by their validation on a larger group of KTx patients with biopsy-proven TAC toxicity. Hopefully, this will help improve clinical outcomes, graft survival rate, dose adjustment and quality of life but also will represent essential tools in guiding therapeutic strategies.

5. Conclusions

Using UHPLC–MS serum profiling and machine learning algorithms we proved that KTx patients with abnormal TAC levels exhibit a particular metabolomic signature that might help diagnose TAC toxicity without graft biopsy based on a panel of five lipid metabolites, serum Mg^{2+}, and UA. Our results need to be further validated with targeted MS on larger cohorts with biopsy-proven TAC toxicity.

Supplementary Materials: The following supporting information can be downloaded at: https://www.mdpi.com/article/10.3390/biomedicines10051157/s1, Figure S1: The relationship between the number of PCs and the explained variability; Table S1: High Tacrolimus Group; Table S2: Metabolite; Table S3: Excel File S1.

Author Contributions: D.B., F.I.E., C.I., A.T., O.A., T.P.K. and T.M. performed the literature research and drafted the manuscript. D.B., F.I.E., A.E., A.M., O.A., I.M.K., and C.S. designed the study. C.S. performed the metabolomic analyses. D.B., C.I., T.M., F.I.E., Ș.D.I. and I.M.K. acquired the data and performed data analysis and interpretation. D.B., C.I., I.M.K., T.M. and A.T. contributed to the overall review of the study and manuscript modification. D.B., I.M.K. and F.I.E. critically revised the manuscript. All authors have read and agreed to the published version of the manuscript.

Funding: This study was funded by a PCD 2020-2021 grant from the "Iuliu Haţieganu" University of Medicine and Pharmacy, Cluj Napoca. Contract Nr. 2461/7 from 17 January 2020.

Institutional Review Board Statement: The study was approved by the Ethics Committee of the Institute of Urology and Kidney Transplantation of Cluj-Napoca, No. 2/2020, and by the Ethics Committee of the Iuliu Hatieganu University of Medicine and Pharmacy in Cluj-Napoca, No. 285/2020.

Informed Consent Statement: Written informed consent was obtained from all patients following the rules and principles of the Helsinki Declaration.

Data Availability Statement: Not applicable.

Conflicts of Interest: The authors declare no conflict of interest.

Abbreviations

6-MP—6-mercaptopurine; ALAT—alanine aminotransferase; AP—Arachidyl palmitoleate (C36:1); AR—acute rejection; ASAT—aspartate aminotransferase; Ca^{2+}—ionized calcium; cdDAG—Cytidine diphosphate diacylglycerol; CER—Ceramide (t18:0/22:0(2OH)); Cl^{-}—chloride; CNI—Calcineurin inhibitors; eGFR—estimated glomerular filtration rate; ER—Endoplasmic reticulum; ESRD—End-stage renal disease; Fn14—Fibroblast growth factor–inducible 14; GGT—gamma-glutamyl transferase; UHPLC—High-precision liquid chromatography; IP3—1,4,5-trisphosphate; ITPR—Inositol 1,4,5-TrisPhosphate Receptor; LCMS—Liquid chromatography–mass spectrometry; K^{+}—potassium; KTx—kidney transplant; Mg^{2+}—Magnesium; MS—Mass spectrometry; Na^{2+}—sodium chloride; PC—Phosphatidylcholine; PE—Phosphatidyl ethanolamine (36:4); PG—Phosphatidyl glycerol (36:6); PI—Phosphatidylinositol; PI3K—Phosphoinositide-3-kinase; PS—Phosphatidyl serine (44:8)—PS (44:8); TAC—Tacrolimus; TP—total proteins; TWEAK—TNF-related weak inducer of apoptosis; UA—Uric acid

References

1. Kostro, J.Z.; Hellmann, A.; Kobiela, J.; Skóra, I.; Lichodziejewska-Niemierko, M.; Dębska-Ślizień, A.; Śledziński, Z. Quality of Life After Kidney Transplanta-tion: A Prospective Study. *Transplantation Proc.* **2016**, *48*, 50–54. [CrossRef] [PubMed]
2. A Kaballo, M.; Canney, M.; O'Kelly, P.; Williams, Y.; O'Seaghdha, C.M.; Conlon, P.J. A comparative analysis of survival of patients on dialysis and after kidney transplantation. *Clin. Kidney J.* **2017**, *11*, 389–393. [CrossRef]
3. Mehdorn, A.S.; Reuter, S.; Suwelack, B.; Schütte-Nütgen, K.; Becker, F.; Senninger, N.; Palmes, D.; Vogel, T.; Bahde, R. Comparison of kidney allograft survival in the Euro-transplant senior program after changing the allocation criteria in 2010—A single center experience. *PLoS ONE* **2020**, *15*, e0235680. [CrossRef] [PubMed]
4. Fabrizii, V.; Kovarik, J.; Bodingbauer, M.; Kramar, R.; Hörl, W.H.; Winkelmayer, W.C. Long-Term Patient and Graft Survival in the Eurotransplant Senior Program: A Single-Center Experience. *Transplantation* **2005**, *80*, 582–589. [CrossRef] [PubMed]
5. Cheungpasitporn, W.; Lentine, K.L.; Tan, J.C.; Kaufmann, M.; Caliskan, Y.; Bunnapradist, S.; Lam, N.N.; Schnitzler, M.; Axelrod, D.A. Immunosuppression Considerations for Older Kidney Transplant Recipients. *Curr. Transplant. Rep.* **2021**, *8*, 100–110. [CrossRef] [PubMed]
6. A. Breda (Chair) KB, K.A. Figueiredo, E. Lledó García, J. Olsburgh (Vice-chair), H. Regele Guidelines Associates: R. Boissier, V. Hevia, O. Rodríguez Faba, R.H. Zakri. Renal Transplantation EAU Guidelines 2021. Available online: https://uroweb.org/guidelines/renal-transplantation/summary-of-changes/2021 (accessed on 1 April 2022).
7. Laskow, D.A.; Vincenti, F.; Neylan, J.F.; Mendez, R.; Matas, A.J. An open-label, concentration-ranging trial of FK506 in primary kidney transplan-tation: A Report of the United States Multicenter FK506 Kidney Transplant Group1. *Transplantation* **1996**, *62*, 900–905. [CrossRef]
8. Pirsch, J.D.; Miller, J.; Deierhoi, M.H.; Vincenti, F.; Filo, R.S. A comparison Of tacrolimus (FK506) and cyclosporine for immuno-suppression after cadaveric renal transplantation1. *Transplantation* **1997**, *63*, 977–983. [CrossRef]
9. Yu, M.; Liu, M.; Zhang, W.; Ming, Y. Pharmacokinetics, pharmacodynamics and pharmacogenetics of tacrolimus in kidney transplantation. *Curr. Drug. Metab.* **2018**, *19*, 513–522. [CrossRef]
10. Issa, N.; Kukla, A.; Ibrahim, H.N. Calcineurin Inhibitor Nephrotoxicity: A Review and Perspective of the Evidence. *Am. J. Nephrol.* **2013**, *37*, 602–612. [CrossRef]
11. Fernando, M.; Peake, P.W.; Endre, Z.H. Biomarkers of calcineurin inhibitor nephrotoxicity in transplantation. *Biomarkers Med.* **2014**, *8*, 1247–1262. [CrossRef]
12. Toole, B.; Gechtman, C.; Dreier, J.; Kuhn, J.; Gutierrez, M.R.; Barrett, A.; Niederau, C. Evaluation of the new cyclosporine and tacrolimus automated elec-trochemiluminescence immunoassays under field conditions. *Clin. Lab.* **2015**, *61*, 1303–1315. [CrossRef]
13. Fujirebio Diagnostics Inc. M, PA. ARCHITECT Tacrolimus April 2009. Available online: https://www.ilexmedical.com/files/PDF/Tacrolimus_ARC.pdf (accessed on 1 April 2022).
14. Araújo, N.C.; Rebelo, M.A.P.; Rioja, L.D.S.; Suassuna, J.H.R. Sonographically determined kidney measurements are better able to predict histological changes and a low CKD-EPI eGFR when weighted towards cortical echogenicity. *BMC Nephrol.* **2020**, *21*, 1–8. [CrossRef] [PubMed]
15. Cusumano, A.M.; Tzanno-Martins, C.; Rosa-Diez, G.J. The Glomerular Filtration Rate: From the Diagnosis of Kidney Function to a Public Health Tool. *Front. Med.* **2021**, *8*. [CrossRef] [PubMed]
16. Toplak, M.; Read, S.T.; Sandt, C.; Borondics, F. Quasar: Easy Machine Learning for Biospectroscopy. *Cells* **2021**, *10*, 2300. [CrossRef] [PubMed]
17. Toplak, M.; Birarda, G.; Read, S.; Sandt, C.; Rosendahl, S.M.; Vaccari, L.; Demšar, J.; Borondics, F. Infrared Orange: Connecting Hyperspectral Data with Machine Learning. *Synchrotron Radiat. News* **2017**, *30*, 40–45. [CrossRef]
18. Pascual, J.; Diekmann, F.; Fernández-Rivera, C.; Marqués, G.G.; Gutiérrez-Dalmau, A.; Pérez-Sáez, M.J.; Sancho-Calabuig, A.; Oppenheimer, F. Recommendations for the use of everolimus in de novo kidney transplantation: False beliefs, myths and realities. *Nefrología (Eng. Ed.)* **2017**, *37*, 253–266. [CrossRef]
19. Gantar, K.; Škerget, K.; Mochkin, I.; Bajc, A. Meeting Regulatory Requirements for Drugs with a Narrow Therapeutic Index: Bioequivalence Studies of Generic Once-Daily Tacrolimus. *Drug Health Patient Saf.* **2020**, *ume 12*, 151–160. [CrossRef]
20. Masuda, S.; Uemoto, S.; Hashida, T.; Inomata, Y.; Tanaka, K.; Inui, K. Effect of intestinal P-glycoprotein on daily tacrolimus trough level in a living-donor small bowel recipient. *Clin. Pharmacol. Ther.* **2000**, *68*, 98–103. [CrossRef]
21. JJoy, M.S.; Hogan, S.L.; Thompson, B.D.; Finn, W.F.; Nickeleit, V. Cytochrome P450 3A5 expression in the kidneys of patients with calcineurin in-hibitor nephrotoxicity. *Nephrol Dial. Transplant.* **2007**, *22*, 1963–1968. [CrossRef]
22. Yanagimachi, M.; Naruto, T.; Tanoshima, R.; Kato, H.; Yokosuka, T.; Kajiwara, R.; Fujii, H.; Tanaka, F.; Goto, H.; Yagihashi, T.; et al. Influence of CYP3A5 and ABCB1 gene polymorphisms on calcineurin inhibitor-related neurotoxicity after hematopoietic stem cell transplantation. *Clin. Transplant.* **2010**, *24*, 855–861. [CrossRef]
23. Bonezi, V.; Genvigir, F.D.V.; Salgado, P.D.C.; Felipe, C.R.; Tedesco-Silva, H., Jr.; Medina-Pestana, J.O.; Cerda, A.; Doi, S.Q.; Hirata, M.H.; Hirata, R.D.C. Differential expression of genes related to calcineurin and mTOR signaling and regulatory miRNAs in peripheral blood from kidney recipients under tacrolimus-based therapy. *Ann. Transl. Med.* **2020**, *8*, 1051. [CrossRef] [PubMed]
24. LiverTox: Clinical and Research Information on Drug-Induced Liver Injury [Internet]. Bethesda (MD): National Institute of Diabetes and Digestive and Kidney Diseases; 2012. Available online: https://www.ncbi.nlm.nih.gov/books/NBK547852/. (accessed on 1 April 2022).

25. Francke, M.I.; Andrews, L.M.; Le, H.L.; van de Wetering, J.; Groningen, M.C.C.; van Gelder, T.; van Schaik, R.H.N.; van der Holt, B.; de Winter, B.C.M.; Hesselink, D.A. Avoiding Tacrolimus Underexposure and Overexposure with a Dosing Algorithm for Renal Transplant Recipients: A Single Arm Prospective Intervention Trial. *Clin. Pharmacol. Ther.* **2021**, *110*, 169–178. [CrossRef] [PubMed]
26. Andrews, L.M.; de Winter, B.C.M.; Cornelissen, E.A.M.; de Jong, H.; Hesselink, D.A.; Schreuder, M.F.; Brüggemann, R.J.M.; van Gelder, T.; Cransberg, K. A Population Pharmacokinetic Model Does Not Predict the Optimal Starting Dose of Tacrolimus in Pediatric Renal Transplant Recipients in a Prospective Study: Lessons Learned and Model Improvement. *Clin. Pharmacokinet.* **2019**, *59*, 591–603. [CrossRef] [PubMed]
27. Wang, P.; Zhang, Q.; Tian, X.; Yang, J.; Zhang, X. Tacrolimus Starting Dose Prediction Based on Genetic Polymorphisms and Clinical Factors in Chinese Renal Transplant Recipients. *Genet. Test. Mol. Biomarkers* **2020**, *24*, 665–673. [CrossRef]
28. Schmitz, V.; Klawitter, J.; Bendrick-Peart, J.; Schoening, W.; Puhl, G.; Haschke, M.; Klawitter, J.; Consoer, J.; Rivard, C.J.; Chan, L.; et al. Metabolic profiles in urine reflect nephrotoxicity of sirolimus and cyclosporine following rat kidney transplantation. *Nephron Exp. Nephrol.* **2009**, *111*, e80–e91. [CrossRef]
29. Klawitter, J.; Bendrick-Peart, J.; Rudolph, B.; Beckey, V.; Klawitter, J.; Haschke, M.; Rivard, C.; Chan, L.; Leibfritz, D.; Christians, U.; et al. Urine Metabolites Reflect Time-Dependent Effects of Cyclosporine and Sirolimus on Rat Kidney Function. *Chem. Res. Toxicol.* **2008**, *22*, 118–128. [CrossRef]
30. Klawitter, J.; Haschke, M.; Kahle, C.; Dingmann, C.; Klawitter, J.; Leibfritz, D.; Christians, U. Toxicodynamic effects of ciclosporin are reflected by metabo-lite profiles in the urine of healthy individuals after a single dose. *Br. J. Clin. Pharmacol.* **2010**, *70*, 241–251. [CrossRef]
31. Klepacki, J.; Klawitter, J.; Klawitter, J.; Thurman, J.M.; Christians, U. A high-performance liquid chromatography–tandem mass spectrometry–based targeted metabolomics kidney dysfunction marker panel in human urine. *Clin. Chim. Acta* **2015**, *446*, 43–53. [CrossRef]
32. Kim, C.-D.; Kim, E.-Y.; Yoo, H.; Lee, J.W.; Ryu, D.H.; Noh, D.W.; Park, S.-H.; Kim, Y.-L.; Hwang, G.-S.; Kwon, T.-H. Metabonomic Analysis of Serum Metabolites in Kidney Transplant Recipients With Cyclosporine A- or Tacrolimus-Based Immunosuppression. *Transplantation* **2010**, *90*, 748–756. [CrossRef]
33. Quaschning, T.; Mainka, T.; Nauck, M.; Rump, L.C.; Wanner, C.; Krämer-Guth, A. Immunosuppression enhances atherogenicity of lipid profile after transplantation. *Kidney Int.* **1999**, *56*, S235–S237. [CrossRef]
34. Agarwal, A.; Prasad, G.V.R. Post-transplant dyslipidemia: Mechanisms, diagnosis and management. *World J. Transplant.* **2016**, *6*, 125–134. [CrossRef] [PubMed]
35. Psychogios, N.; Hau, D.D.; Peng, J.; Guo, A.C.; Mandal, R.; Bouatra, S.; Sinelnikov, I.; Krishnamurthy, R.; Eisner, R.; Gautam, B.; et al. The human serum metabolome. *PLoS ONE* **2011**, *6*, e16957. [CrossRef] [PubMed]
36. Riella, L.V.; Gabardi, S.; Chandraker, A. Dyslipidemia and its therapeutic challenges in renal transplantation. *Am. J. Transplant.* **2012**, *12*, 1975–1982. [CrossRef] [PubMed]
37. Zhang, B.; Kuipers, F.; de Boer, J.F.; Kuivenhoven, J.A. Modulation of Bile Acid Metabolism to Improve Plasma Lipid and Lipoprotein Profiles. *J. Clin. Med.* **2021**, *11*, 4. [CrossRef]
38. Hishikawa, D.; Hashidate, T.; Shimizu, T.; Shindou, H. Diversity and function of membrane glycerophospholipids generated by the remodeling pathway in mammalian cells. *J. Lipid Res.* **2014**, *55*, 799–807. [CrossRef]
39. Yang, Y.; Lee, M.; Fairn, G.D. Phospholipid subcellular localization and dynamics. *J. Biol. Chem.* **2018**, *293*, 6230–6240. [CrossRef]
40. Karolin, A.; Escher, G.; Rudloff, S.; Sidler, D. Nephrotoxicity of Calcineurin Inhibitors in Kidney Epithelial Cells is Independent of NFAT Signaling. *Front. Pharmacol.* **2022**, *12*. [CrossRef]
41. Claus, M.; Herro, R.; Wolf, D.; Buscher, K.; Rudloff, S.; Huynh-Do, U.; Burkly, L.; Croft, M.; Sidler, D. The TWEAK/Fn14 pathway is required for calcineurin inhibitor toxicity of the kidneys. *Am. J. Transplant.* **2017**, *18*, 1636–1645. [CrossRef]
42. Blassberg, R.; Jacob, J. Lipid metabolism fattens up hedgehog signaling. *BMC Biol.* **2017**, *15*, 1–14. [CrossRef]
43. Taniguchi, M.; Okazaki, T. Ceramide/sphingomyelin rheostat regulated by sphingomyelin synthases and chronic diseases in murine models. *J. Lipid Atheroscler.* **2020**, *9*, 380. [CrossRef] [PubMed]
44. Chaurasia, B.; Summers, S.A. Ceramides–lipotoxic inducers of metabolic disorders. *Trends Endocrinol. Metab.* **2015**, *26*, 538–550.
45. Mather, A.R.; Siskind, L.J. Glycosphingolipids and Kidney Disease. *Sphingolipids Metab. Dis.* **2011**, *721*, 121–138. [CrossRef]
46. Lee, A.M.; Hu, J.; Xu, Y.; Abraham, A.G.; Xiao, R.; Coresh, J.; Rebholz, C.; Chen, J.; Rhee, E.P.; Feldman, H.I.; et al. Using Machine Learning to Identify Metabolomic Signatures of Pediatric Chronic Kidney Disease Etiology. *J. Am. Soc. Nephrol.* **2022**, *33*, 375–386. [CrossRef]
47. Navaneethan, S.D.; Sankarasubbaiyan, S.; Gross, M.D.; Jeevanantham, V.; Monk, R.D. Tacrolimus-associated hypomagnesemia in renal transplant recipients. *Transplant. Proc.* **2006**, *38*, 1320–1322. [CrossRef] [PubMed]
48. Rodrigues, N.; Santana, A.; Guerra, J.; Neves, M.; Nascimento, C.; Gonçalves, J.; da Costa, A. Serum Magnesium and Related Factors in Long-Term Renal Transplant Recipients: An Observational Study. *Transplant. Proc.* **2017**, *49*, 799–802. [CrossRef]
49. Gratreak, B.; Swanson, E.; Lazelle, R.A.; Jelen, S.K.; Hoenderop, J.; Bindels, R.J.; Yang, C.; Ellison, D.H. Tacrolimus-induced hypomagnesemia and hypercalciuria requires FKBP12 suggesting a role for calcineurin. *Physiol. Rep.* **2020**, *8*, e14316. [CrossRef]
50. Kanbay, M.; Akcay, A.; Huddam, B.; Usluogullari, C.; Arat, Z.; Ozdemir, F.; Haberal, M. Influence of Cyclosporine and Tacrolimus on Serum Uric Acid Levels in Stable Kidney Transplant Recipients. *Transplant. Proc.* **2005**, *37*, 3119–3120. [CrossRef]

51. Chang, H.; Lin, C.; Lian, J. Predictors of Renal Function Improvement Following Tacrolimus Conversion in Cyclosporine-Treated Kidney Transplant Recipients. *Transplant. Proc.* **2007**, *39*, 3135–3141. [CrossRef]
52. Diémé, B.; Halimi, J.M.; Emond, P.; Büchler, M.; Nadal-Desbarat, L.; Blasco, H.; Le Guellec, C. Assessing the Metabolic Effects of Calcineurin Inhibitors in Renal Transplant Recipients by Urine Metabolic Profiling. *Transplantation* **2014**, *98*, 195–201. [CrossRef]
53. Zhang, F.; Wang, Q.; Xia, T.; Fu, S.; Tao, X.; Wen, Y.; Chan, S.; Gao, S.; Xiong, X.; Chen, W. Diagnostic value of plasma tryptophan and symmetric dimethylarginine levels for acute kidney injury among tacrolimus-treated kidney transplant patients by targeted metabolomics analysis. *Sci. Rep.* **2018**, *8*, 14688. [CrossRef] [PubMed]